Laser Synthesis and Luminescence Properties of $SrAl_2O_4:Eu^{2+}$, Dy^{3+} Phosphors

Raquel Aroz [a], Vassili Lennikov [a,*], Rafael Cases [b], María Luisa Sanjuán [a], Germán F. de la Fuente [a], Edgar Muñoz [c,*]

[a] *Instituto de Ciencia de Materiales de Aragón, CSIC-Universidad de Zaragoza, Zaragoza, Spain*

[b] *Departamento de Física de la Materia Condensada, Instituto de Ciencia de Materiales de Aragón, CSIC-Universidad de Zaragoza, Pedro Cerbuna 12, 50009 Zaragoza, Spain*

[c] *Instituto de Carboquímica ICB-CSIC, Miguel Luesma Castán 4, 50018 Zaragoza, Spain*

* Corresponding authors.

E-mail address: lennikov@unizar.es (V. Lennikov), edgar@icb.csic.es (E. Muñoz).

Abstract

A laser melting method has been developed for the synthesis of highly luminescent, long-lasting $SrAl_2O_4:Eu^{2+}$, Dy^{3+} phosphors. The high temperature achieved in high-power density CO_2 laser irradiation of mixtures of $SrCO_3$, Al_2O_3, Eu_2O_3, and Dy_2O_3 enabled the one-step, fast synthesis of these phosphors in air at atmospheric pressure. X-ray diffraction, Raman spectroscopy, and Scanning Electron Microscopy

characterization studies reveal that the produced materials consist of monoclinic $SrAl_2O_4$ grains extensively surrounded by rare-earth ion-enriched grain boundaries. The photoluminescence properties of laser-produced $SrAl_2O_4:Eu^{2+}$, Dy^{3+} materials are discussed. The results reported here suggest that this laser melting method is a promising route for the synthesis of ceramic phosphors. It is presented as an alternative to the conventional sol-gel- and solid-state methods, which require the use of high-temperature furnaces, flux additives, and reducing atmospheres.

Keywords: Laser melting; Electron microscopy; Spectroscopy; $SrAl_2O_4$; Functional applications

1. Introduction

The luminescence properties of europium-doped alkaline earth aluminates (MAl_2O_4, M=Mg, Ca, Sr, Ba), mainly of $SrAl_2O_4:Eu^{2+}$, have attracted much attention since the pioneering work of Palilla *et al.*[1] Upon exposure to UV light, this ceramic phosphor shows a greenish emission peaking at 520 nm associated to the parity-allowed transition $4f^6\ 5d \rightarrow 4f^7$ of Eu^{2+}. Maruyama *et al.* discovered the outstanding, long-lasting afterglow properties of $SrAl_2O_4:Eu^{2+}, Dy^{3+}$ as a result of the auxiliary activator role of Dy^{3+}.[2] The enhanced brightness and long-persistence properties at room temperature remain for hours, even throughout the whole night. This fact, coupled with the excellent chemical stability, as well as the non-toxic and non-radioactive nature of these materials, has resulted in unprecedented success of these phosphors for applications as luminescent pigments. They are used in safety and emergency signs, as well as in luminous markings in watches and other instruments' dials. $SrAl_2O_4:Eu^{2+}$,

Dy^{3+} phosphors have replaced the previous pigment technology based on ZnS:Cu, which is extremely sensitive to moisture and chemically unstable.[3] The $SrAl_2O_4:Eu^{2+}$, Dy^{3+} phosphor exhibits presently the most persistent after-glowing properties among strontium aluminates and silicates doped with Eu^{2+} and other R^{3+} rare earth ions.[4,5]

The conventional synthesis method of the rare earth activated strontium aluminates is the thermally-driven solid state reaction of Al_2O_3 and $SrCO_3$. This process requires temperatures above 1250ºC because, at this temperature, the stable intermediate $Sr_3Al_2O_6$ phase that quenches the photoluminescence of $SrAl_2O_4$-based pigments is completely transformed into pure $SrAl_2O_4$.[6] Hence, these solid state synthesis routes usually involve the addition of a flux such us B_2O_3 or H_3BO_3. Additionally, a reducing atmosphere is necessary to control the valence of the activator (in this case Eu^{2+} is required instead of Eu^{3+}).[2,7] Alternatively, sol-gel methods have been developed to yield these ceramic phosphors at lower sintering temperatures.[8,9] Variants of Pechini´s sol-gel method have, in addition, been developed where no reducing atmosphere is needed to convert Eu^{3+} to Eu^{2+}.[10,11] However, the long synthesis time required in those methods limits their industrial use. Thus, in recent years other methods such as coprecipitation,[12] sol-gel-microwave processes,[13] as well as hydrothermal and combustion methods [14,15] have been successfully developed to produce strontium aluminate phosphors at lower synthesis temperatures and within shorter reaction times.

In a further significant step, Katsumata *et al.* reported the growth of $SrAl_2O_4$- and $CaAl_2O_4$-based phosphor crystals by means of a floating zone furnace, which through ellipsoidal mirrors is able to locally provide the required temperature for the melting of the precursors used.[16] Laser heating can also be utilized to achieve these extreme high temperature conditions for the efficient, in-situ pigment synthesis directly obtained in ceramic substrates.[17] Thus, our group has pioneered the development of a

convenient laser zone melting method, demonstrating capability for in-plane texture control in Al_2O_3-ZrO_2-based eutectics,[18] in Bi oxide superconductors,[19,20] and lately for surface processing of ceramic tiles to control their structural properties.[21] In addition, the in-situ synthesis of $MTiO_3$ (M = Ca, Sr, Ba) coatings on Al_2O_3 substrates by laser melting of MCO_3 and TiO_2 powder mixtures has also been demonstrated.[22] This laser assisted synthesis is based upon the thermal effects caused by the laser radiation absorbed by the material. It can thus be considered as a photothermal synthetic route, where temperatures well above 2000 ºC may be reached. Hence, the preparation of high melting point oxides has been successfully achieved by using this laser melting method, as demonstrated with the synthesis of ZrO_2 based pigments [23] and, most recently, with the preparation of large, crack-free surface molten eutectics [24] and with the in-situ synthesis of rare earth aluminate perovskite and garnet based eutectic coatings.[25]

In the present work, $SrAl_2O_4$ and $SrAl_2O_4$:Eu^{2+}, Dy^{3+} phosphors with remarkable luminescence properties have been efficiently synthesized by this laser melting method, in a fast single step, directly from their precursors in air at atmospheric pressure. Only monoclinic $SrAl_2O_4$ has been detected in characterization studies performed in materials synthesized by this versatile laser melting method. The phase composition, microstructure, and phase formation, as well as the luminescence properties and mechanisms of the Eu^{2+} and Dy^{3+} doped samples are also investigated and discussed here.

2. Experimental

Commercial $SrCO_3$ (Aldrich, 99.8%), Al_2O_3 (Aldrich, 99.9%), Eu_2O_3 (Aldrich, 99.9%) and Dy_2O_3 (Aldrich, 99.9%) powders were used as the starting materials

according to the nominal composition of $SrAl_2O_4$ (SA), $SrAl_2O_4:Eu_{0.01}$ (SAE) and $SrAl_2O_4:Eu_{0.01}Dy_{0.02}$ (SAED). The starting materials were dried and mixed using a Retch 2000 Ball Mill for 1h using isopropyl alcohol as a liquid suspension medium at 250 rpm. The powder mixture obtained after drying of the resultant suspension was used for the laser synthesis.

The experimental setup used for the laser synthesis is shown in Fig. 1. A Rofin Sinar pulsed CO_2 laser with SLAB type resonator was used as energy source with a maximum nominal power of 350W at 20 kHz. The precursor powder mixture was placed into a refrigerated 70x35 cm aluminium crucible (4), and then scanned with the laser in a thin-line beam configuration (3) at a traverse speed of 5.6 mm/s. The effective focal distance of the lens system used was 950 mm, resulting in a 0.8mm diameter laser spot at its focus.

The crystal structure and crystalline phase composition of the products were characterized by X-ray diffraction (XRD, Cu*K*α radiation λ=1.54056 Å, Bruker D8 Advance series 2). Differential scanning calorimetry (DSC) analyses have been carried out using a SDT Q600 calorimeter (TA instruments) at a heating rate of 10ºC/min. The microstructure and elemental composition of the phosphors were characterized by scanning electron microscopy (SEM JEOL JSM-6400 microscope) with energy dispersive X-ray spectroscopy (EDX). Raman spectroscopy measurements were performed at RT in a DILOR XY spectrometer equipped with a liquid nitrogen cooled CCD detector and excitation through a microscope, using the 514.5 nm line of an Ar^+ laser (model Coherent INNOVA 305). The Si Raman line at 520 cm^{-1} was used for wavelength calibration of the Raman lines.

The functional luminescent parameters of Eu^{2+} and Dy^{3+} doped samples were studied by optical spectroscopy including excitation and emission spectra, as well as

decay curves. Fluorescence emission and excitation spectra were obtained at RT by exciting the samples with a 1000W ORIEL 66187 tungsten halogen lamp and a double 0.22 m SPEX 1680B monochromator. For the emission spectra, the excitation was carried out at 360 nm. For the excitation spectra the emission was detected at 520nm using a 0.5 JARREL-ASH monochromator with a Hamamatsu R928 photomultiplier tube. All optical spectroscopy measurements were corrected from the system response. Emission decay curves were obtained by pulse excitation with a N_2 pumped dye laser (pulse duration 2ns). Lifetime measurements were carried out using a digital storage oscilloscope triggered by the laser.

3. Results and discussion

The laser melting method reported here yields roughly 0.5 g of product per second. The material obtained has a granular appearance, as expected for a polycrystalline material obtained at a relatively fast solidification rate from a melt. Fig. 2 shows photographs of doped $SrAl_2O_4$ phosphors sinthesized by this laser method. An afterglow image of $SrAl_2O_4:Eu^{2+}$, Dy^{3+} is shown in Fig. 2b, where the greenish emission is clearly observed when UV illumination is removed. $SrAl_2O_4:Eu^{2+}$ afterglow, however, can only be perceived upon UV illumination.

The crystalline phase composition of the synthesized phosphors has been analyzed by XRD (Fig. 3). The diffraction peaks can be indexed to a monoclinic $SrAl_2O_4$ phase (JCPDS 34–0379). These results are consistent with the fact that phase changes due to substitution by rare earth ions are not detected by this technique, particularly at the typically low percentage levels of doping required for the observation of efficient luminescence. Within sensitivity of XRD, no secondary phases were detected.

$SrAl_2O_4$ has hexagonal and monoclinic polymorphs: high-temperature and low temperature phases, respectively. It is usually claimed that only the monoclinic phase of $SrAl_2O_4$ shows luminescence properties when doped with rare-earth ions.[7] As mentioned above, the synthesis of pure $SrAl_2O_4$ by solid state methods requires temperatures of ca. 1300ºC. Some studies confirm that the addition of boron oxide as a flux is necessary to stabilize the monoclinic polymorph and some sol-gel methodology also requires the introduction of boron in the phosphor composition.[11] In contrast, the present laser zone melting method yields pure monoclinic $SrAl_2O_4$ without the addition of any flux. Furthermore, XRD patterns indicate that the products synthesized are all $SrAl_2O_4$ monoclinic phase, since no lines from other impurity structures, such as $Sr_4Al_{14}O_{25}$ or $Sr_3Al_2O_6$ low-temperature phases, have been detected.

This point is confirmed by DSC measurements. DSC of $SrAl_2O_4:Eu^{2+}$, Dy^{3+} exhibits a peak at around 660ºC corresponding to the transition from the monoclinic to the hexagonal phase (Fig. 4), in accordance with Ito et al.[26] These results suggest that the monoclinic phase is present in all of the materials obtained via laser melting, although the presence of hexagonal phase cannot be fully discarded, due to the difficulty in distinguishing the monoclinic (2 2 0) from the hexagonal (1 0 2) peak at around 29° in XRD patterns. Raman spectroscopy has then been performed to confirm that the monoclinic phase does not coexist with the hexagonal polymorph.

Fig. 5 compares the Raman spectrum of the $SrAl_2O_4$ material produced by the laser melting method to that of a monoclinic $SrAl_2O_4$ ($P2_1$ space group) reference sample synthesized by conventional solid state reaction.[11] It is clear that both spectra present the same peaks, which confirms that the material produced by laser melting exhibits the $P2_1$ monoclinic structure. No hint of hexagonal $SrAl_2O_4$ was found, using the spectrum of hexagonal, high-temperature $SrAl_2O_4$ as a reference.[27] Measurements

were recorded through the X50 objective lens of a microscope with the Raman laser focused on the center of each single grain observed. While the synthesized material is polycrystalline, in these conditions of Raman spectra collection the spatial resolution (~2 μm) is considerably below the mean grain size (~10 μm), which allows us to assume that we are in fact exploring a single crystal of $SrAl_2O_4$. As the inset of Fig. 5 shows, polarization properties exist, denoting good crystallinity, though a precise mode assignment could not be made since the plane orientation was unknown. Mode polarization explains why the relative band intensities in spectra belonging to single or polycrystalline samples are not identical. In these experiments no evidence for phase segregation was observed; nor were compositional changes at or near the grain boundaries ascertained.

Raman spectra of pure and Eu, Dy-doped $SrAl_2O_4$ are shown in Fig. 6. It is again clear that both pertain to the same monoclinic phase, though the spectrum of doped $SrAl_2O_4$ is more noisy and presents a background that we attribute to luminescence arising from Eu^{2+}, excited by the Raman spectrometer laser at 514.5 nm.

SEM micrographs of the synthesized $SrAl_2O_4$:Eu^{2+}, Dy^{3+} phosphors (Fig. 7a) illustrate the granular microstructure of this material. Backscattered SEM micrographs of the synthesized $SrAl_2O_4$:Eu^{2+}, Dy^{3+} phosphors (Fig. 7b) show grey contrast grains, with an average size of about 10 μm, sourronded by a lighter grey contrast phase which contains higher rare-earth ion concentration per volume, as revealed by EDX. Based on these EDX elemental analyses data, measured at the grains and the grain boundaries, phase compositions were asigned to $SrAl_2O_4$ and $SrAl_2O_4$-$SrAl_4O_7$ eutectic, respectively.

The formation of these different phases within these laser-synthesized materials can be explained as follows: the precursor powder mixture is laser-heated instantly to a

liquid, molten state, inducing subsequent chemical reactions between the components present. The compositions of the starting mixtures were calculated by substitution of $SrCO_3$ with the corresponding amount of rare earth oxide, expecting that the last should replace Ca positions in the $SrAl_2O_4$ crystal lattice. As a result, the real composition of the melt formed shifts towards the $SrAl_2O_4$-$SrAl_4O_7$ eutectic in the SrO-Al_2O_3 phase diagram.[28] Once the laser irradiation ceases, the temperature of this melt decreases along to the liquidus curve at 1960 ºC, resulting in the crystallization of the $SrAl_2O_4$ phase. The eutectic melt and solid $SrAl_2O_4$ coexist until the eutectic temperature is reached (1660 ºC). Thus, the eutectic system acts as a flux, allowing the growth of $SrAl_2O_4$ phase grains. As a result, the rare earth ions are rejected to the eutectic melt that solidifies around the main grains below the eutectic temperature, just as the micrograph appearing in Fig. 8a suggests, with the build-up of a white contrast layer within the intergranular space (this build-up of Eu and Dy cations at the grain boundaries has been confirmed by EDX measurements). Further evidence for eutectic formation was also confirmed by the presence of lamellar structures in SEM micrographs (Fig. 8b). These lamellae are characteristic of directionally solidified eutectic systems.[29]

Excitation and emission spectra of $SrAl_2O_4$:Eu^{2+} are shown in Fig. 9. Quite similar spectra have been collected for $SrAl_2O_4$: Eu^{2+}, Dy^{3+}. Both phosphors present a broad excitation band and a broad emission band peaking at λ=520nm atributted to the interconfigurational transition from the $4f^6\ 5d^1$ excited state to the $4f^7$ (^8S) ground state of Eu^{2+} ions.[30]

Monoclinic $SrAl_2O_4$ belongs to the stuffed tridymite type structure, where two different Sr^{2+} sites with similar local distortion are present. As Sr^{2+} and Eu^{2+} have very similar ionic radii, the occupation of the Sr^{2+} sites by Eu^{2+} is expected. Thus, the

greenish emission is attributed to Eu^{2+} located inside the host lattice. The width of the bands confirms this result as it is due to the splitting of the mixed 4f5d state by the crystal field of the host lattice. Furthermore, no emission peaks in the red region from the characteristic intraconfigurational transition 4f $\rightarrow$ 4f of Eu^{3+} have been detected, indicating that the rare earth ions that have not diffused remain as divalent europium ions in the grain boundaries. Here, their concentration is so high in comparison to the reduced area of grain boundaries, that the emission from these Eu^{2+} ions could be largely quenched, resulting in shorter lifetime values than those corresponding to Eu^{2+} ions located inside the grains. On the other hand, the wavelength of the emission band does not vary from $SrAl_2O_4$:Eu^{2+} to $SrAl_2O_4$: Eu^{2+}, Dy^{3+}. The luminescent centers are Eu^{2+} ions, and no additional emission band assigned to Dy^{3+} is found in $SrAl_2O_4$: Eu^{2+}, Dy^{3+}. As expected, only the phosphors co-doped with Dy^{3+} exhibit significant long-lasting afterglow properties.[2]

Decay curves of the afterglow of $SrAl_2O_4$:Eu^{2+} and $SrAl_2O_4$: Eu^{2+}, Dy^{3+} samples at room temperature are depicted in Fig. 10. The luminescence decay process of the samples is nonexponential. Both decay processes of luminescence undergo an initial fast decay (not shown), followed by a slow decaying process which accounts for the observed long-lasting phosphorescence. The fast decay process corresponds to the intrinsic lifetime of Eu^{2+}. The slower decay process, which is significant only in $SrAl_2O_4$: Eu^{2+}, Dy^{3+} samples, is attributed to the presence of Dy^{3+} ions into the host lattice.

The measured luminescent properties of the phosphors synthesized by this novel laser melting method can be explained in terms of the thermally-activated hole trapping and detrapping mechanism proposed by Matsuzawa et al.[2,31] Based on it, the Dy^{3+} ions act as deep hole trapping centers. Upon UV-light exposure, Eu^{2+} excitation occurs as a

result of the electron transition from 4f to 4f5d state, leading to a hole at the 4f ground state level which is thermally released to the valence band at room temperature. The released hole migrates through the valence band until Dy^{3+} traps it, so it is assumed that Eu^{2+} is converted into Eu^{+} and Dy^{3+} into Dy^{4+}. When UV excitation ends, the reversed route and the recombination of holes and electrons occurs leading to the measured bright and long-lasting phosphorescence.

4. Conclusions

A laser melting method is described for the efficient synthesis of strontium aluminates with the composition $SrAl_2O_4$ and related phosphors. The phosphors obtained by this method present the appropriate monoclinic phase structure, with a satisfactory fit for good luminescent properties. The advantages of this method over conventional methods include fast material synthesis in the absence of reducing atmospheres and simple precursor preparation. This versatile laser zone melting method may thus enable the synthesis of other phosphors and a whole plethora of other functional oxides and inorganic materials.

Acknowledgments

The authors acknowledge financial support from the Spanish Ministry of Science and Innovation (MICINN, projects CEN-20072014 and MAT2010-19837-C06-06), IMPLASER 99 S.L.L. (www.implaser.com), and the regional Government of Aragón (Spain, project PI119/09, and Excellence Research Groups Program T87).

References

1. Palilla FC, Levine AK, Tomkus MR. Fluorescent properties of alkaline earth aluminates of type MAl_2O_4 activated by divalent europium. *J Electrochem Soc* 1968;**115**:642-4.

2. Matsuzawa T, Aoki Y, Takeuchi N, Murayama Y. New long phosphorescent phosphor with high brightness, $SrAl_2O_4:Eu^{2+},Dy^{3+}$. *J Electrochem Soc* 1996;**143**:2670-3.

3. Swart HC. A review on ZnS phosphor degradation. *Phys Stat Sol C* 2004;**9**:2354-9.

4. Clabau F, Rocquefelte X, Jobic S, Deniard P, Whangbo MH, Garcia A, et al. On the phosphorescence mechanism in $SrAl_2O_4 : Eu^{2+}$ and its codoped derivatives. *Solid Sta Sci* 2007;**9**:608-12.

5. Lakshminarasimhan N, Varadaraju UV. Luminescence and afterglow in $Sr_2SiO_4:Eu^{2+}$, RE^{3+} [RE = Ce, Nd, Sm and Dy] phosphors-Role of co-dopants in search for afterglow. *Mat Res Bull* 2008;**43**:2946-53.

6. Song YK, Choi SK, Moon HS, Kim TW, Mho S-I, Park HL. Phase studies of SrO-Al_2O_3 by emission signatures of Eu^{2+} and Eu^{3+}. *Mat Res Bull* 1997**;32**:337-41.

7. Sánchez-Benítez J, de Andrés A, Marchal M, Cordoncillo E, Vallet Regi M, Escribano P. Optical study of $SrAl_{1.7}B_{0.3}O_4 : Eu, R$ (R = Nd, Dy) pigments with long-lasting phosphorescence for industrial uses. *J Solid State Chem* 2003;**171**:273-7.

8. Chen I-C, Chen T-M. Sol-gel synthesis and the effect of boron addition on the phosphorescent properties of $SrAl_2O_4 : Eu^{2+},Dy^{3+}$ phosphors. *J Mater Res* 2001**;16**:644-51.

9. Peng T, Huajun L, Yang H, Yan C. Synthesis of $SrAl_2O_4$: Eu,Dy phosphor nanometer powders by sol-gel processes and its optical properties. *Mat Chem Phys* 2004;**85**:68-72.

10. Marchal M, Escribano P, Carda JB, Cordoncillo E. Long-lasting phosphorescent pigments of the type $SrAl_2O_4$: Eu^{2+},R^{3+}(R = Dy, Nd) synthesized by the sol-gel method. *J Sol-Gel Sci Tech* 2003;**26**:989-92.

11. Escribano P, Marchal M, Sanjuán ML, Alonso-Gutiérrez P, Julián B, Cordoncillo E. Low-temperature synthesis of $SrA1_2O_4$ by a modified sol-gel route: XRD and Raman characterization. J *Solid State Chem* 2005;**178**:1978-97.

12. Choi S-H, Kim N-H, Yun Y-H, Choi S-C. Photoluminescence properties of $SrAl_2O_4$ and $CaAl_2O_4$ long-phosphorescent phosphors synthesized by an oxalate coprecipitation method *J Ceram Proc Res* 2006;**7**:62-5.

13. Wu S, Zhang S, Yang J**.** Influence of microwave process on photoluminescence of europium-doped strontium aluminate phosphor prepared by a novel sol–gel-microwave process. *Mat Chem Phys* 2007;**102**:80-5.

14. Peng T, Yang H, Pu X, Hu B, Jiang Z, Yan C. Combustion synthesis and photoluminescence of $SrAl_2O_4$:Eu,Dy phosphor nanoparticles. *Mater Lett* 2004;**58**:352-6.

15. Zhang R, Han G, Zhang L, Yan B. Gel combustion synthesis and luminescence properties of nanoparticles of monoclinic $SrAl_2O_4$:Eu^{2+},Dy^{3+}. *Mat Chem Phys* 2009;**113**:255-9.

16. Katsumata T, Sakai R, Komuro S, Morikawa T, Kimura H. Growth and characteristics of long duration phosphor crystals. *J Crystal Growth* 1999;**198-9**:869-71.

17. Bakali J, Fortanet E, de la Fuente X, Lahoz R, Estepa LC, Peris G, et al. Structural and microstructural characterisation of refractory oxides synthesised by laser. *Key Eng Mater* 2004;**264-8**:317-20.

18. Larrea A, de la Fuente GF, Merino RI, Orera VM. ZrO_2-Al_2O_3 eutectic plates produced by laser zone melting. *J Eur Ceram Soc* 2002**;22**:191-8.

19. Mora M, Díez JC, López-Gascón CI, Martínez E de la Fuente GF. Laser textured Bi-2212 in planar geometries. *IEEE Trans Appl Supercon* 2003;**13**:3188-91.

20. Lennikov VV, Kazin PE, Tretyakov YD**,** de la Fuente GF. Laser Zone Melting and Texture Formation in MgO-doped $Bi_{2.03}Sr_{1.93}Ca_{1.07}Cu_{2.05}O_{8+\delta}$. *Z Anorg Allg Chem* 2004;**630**:2337-42.

21. Gutiérrez-Mora F, Domínguez-Rodríguez A, Lennikov VV, de la Fuente GF. Influence of thermal effects produced by laser treatment on the tribological behavior of porcelain ceramic tiles. *Key Eng Mater* 2010;**423**:41-46.

22. Lennikov VV, Pedra JM, Gómez JJ, de la Fuente GF, Carda JB. In situ synthesis of composite $MTiO_3$-Al_2O_3 coatings via laser zone melting. *Solid State Sci* 2007;**9**:404-9.

23. Nebot A, Goyeneche I, Jovani MA, Lennikov VV, Lahoz R, Estepa LC, et al. "Desarrollo de materiales cerámicos utilisando technología láser" *Proc of IX World Congress on Ceramic Tile Quality - Qualicer'06:* 2006, C. P.BC-23 - P.BC-34.

24. Gurauskis J, Lennikov V, de la Fuente GF, Merino RI. Laser-assisted, crack-free surface melting of large eutectic ceramic bodies. *J Eur Ceram Soc* 2011;**31**:1251-6.

25. de Francisco I, Lennikov VV, Bea JA, Vegas A, Carda JB, de la Fuente GF. In-situ laser synthesis of rare earth aluminate coatings in the system Ln-Al-O (Ln = Y, Gd). *Solid State Sci* 2011;**13**:1813-9.

26. Ito S, Banno S, Suzuki K, Inagaki M. Phase transition in $SrAl_2O_4$. *Z Physik Chem* 1977;**105**:173-8.

27. Cordoncillo E, Julián-López B, Martínez M, Sanjuán ML, Escribano P. New insights in the structure–luminescence relationship of Eu:$SrAl_2O_4$. *J Alloys Comp* 2009**;484**:693-7.

28. Ganits F, Chemekova TY, Udalov YP. Strontium oxide - alumina system. *Zh Neorg Khim* 1979; **24**; 471-5.

29. Llorca J, Orera VM. Directionally solidified eutectic ceramic oxides. *Prog Mater Sci* 2006; **51**:711-809.

30. Blasse G, Grabmaier BC. *Luminescent Materials,* Springer;1994.

31. Yamamoto H, Matsuzawa T. Mechanism of long phosphorescence of $SrA1_2O_4$: Eu^{2+}, Dy^{3+} and $CaAl_2O_4$: Eu^{2+}, Nd^{3+}. *J Lumin* 1997;**72**:287.

Figure Captions

Fig. 1. Experimental laser synthesis apparatus employed for this work: laser source (1), beam steering system (2), laser beam steering zone (3), laser-surface modified aluminium crucible (4).

Fig. 2. $SrAl_2O_4$: Eu^{2+}, Dy^{3+} phosphor synthesized by laser melting method (a). Glow-image after UV-light exposure (b).

Fig. 3. XRD patterns of $SrAl_2O_4$ (a), $SrAl_2O_4$: Eu^{2+} (b) and $SrAl_2O_4$: Eu^{2+}, $Dy3^{+}$ (c). The $SrAl_2O_4$ JCPDS pattern is shown on the bottom for comparison purposes.

Fig. 4. DSC plot obtained for a $SrAl_2O_4$: Eu^{2+}, Dy^{3+} phosphor prepared by laser melting. The peak observed near 660 ºC is assigned to the monoclinic to hexagonal phase transition reported in the literature for this system.[21]

Fig. 5. Raman spectrum of laser synthesized $SrAl_2O_4$ (lower graph), compared to that of reference monoclinic $SrAl_2O_4$ produced by solid state reaction (upper graph). The inset shows the spectrum of $SrAl_2O_4$ in two different polarization configurations (see text).

Fig. 6. Raman spectra of pure (1) and Eu, Dy doped (2) $SrAl_2O_4$ single crystals.

Fig. 7. SEM micrographs, secondary-electron image (a) and backscattered-electron image (b), showing the microstructure of $SrAl_2O_4$: Eu^{2+}, Dy^{3+} phosphor obtained by

laser melting. Accumulation of heavier (white contrast in backscattered mode) rare earth elements at the grain boundaries is clearly distinguished in (b).

Fig. 8. SEM micrograph of unpolished $SrAl_2O_4:Eu^{2+}$, Dy^{3+} phosphor obtained by the laser melting method, showing the lamellar microstructure of the eutectic phase at different magnifications.

Fig. 9. Emission and excitation spectra of the $SrAl_2O_4$: Eu^{2+} phosphor.

Fig. 10. Decay curves of luminescence of $SrAl_2O_4$: Eu^{2+} (SAE) and $SrAl_2O_4$: Eu^{2+}, Dy^{3+} (SAED) phosphors.

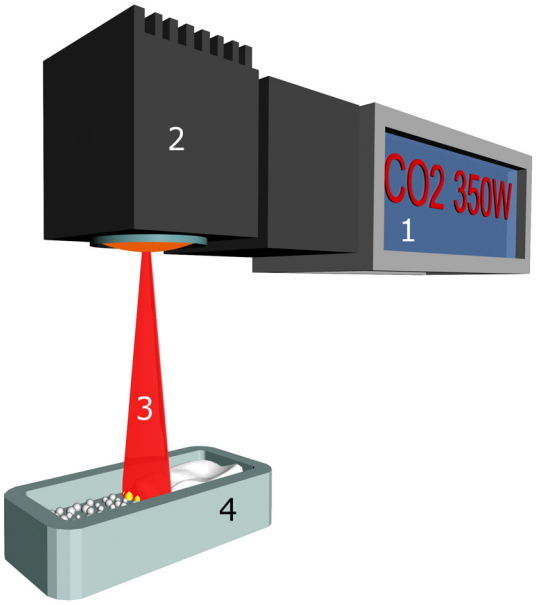

Fig. 1. Experimental laser synthesis apparatus employed for this work: laser source (1), beam steering system (2), laser beam steering zone (3), laser-surface modified aluminium crucible (4).

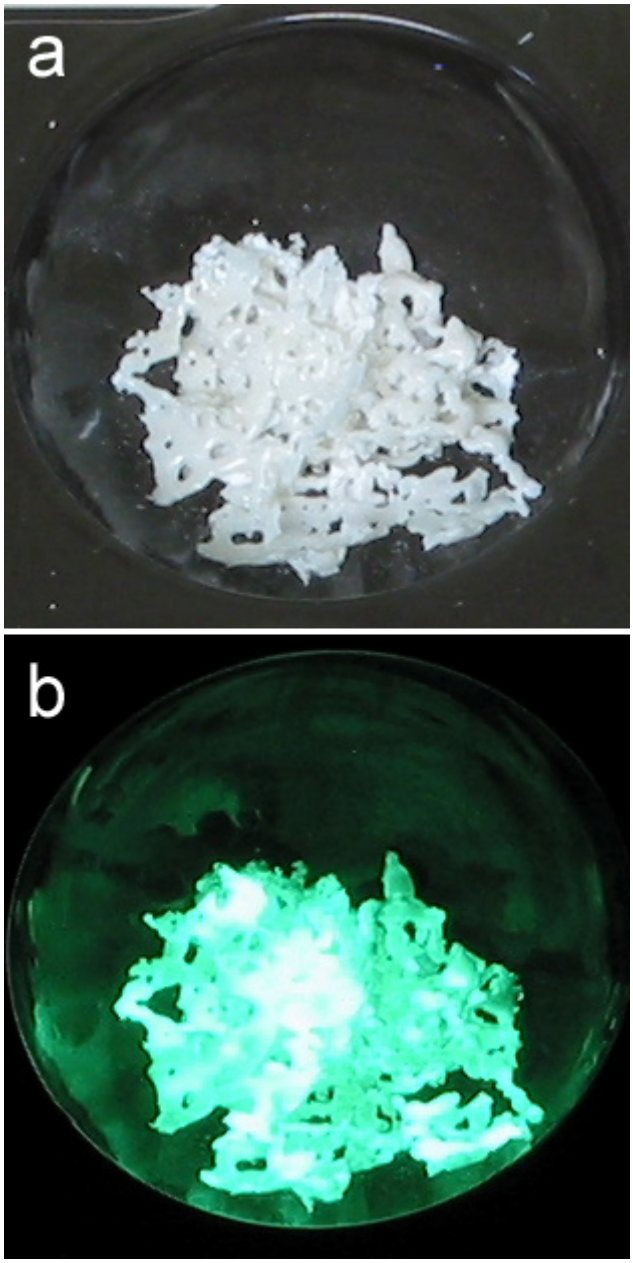

Fig. 2. $SrAl_2O_4$: Eu^{2+}, Dy^{3+} phosphor synthesized by laser melting method (a). Glow-image after UV-light exposure (b).

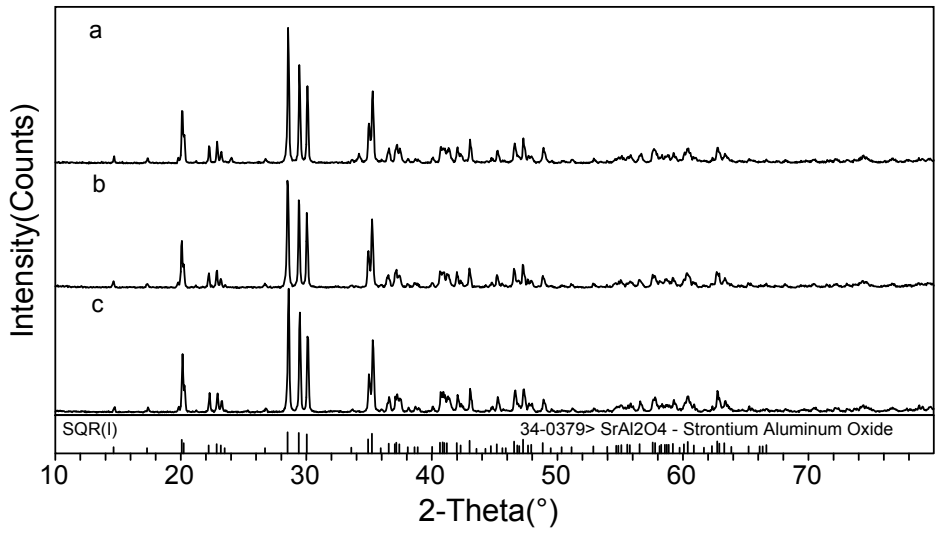

Fig. 3. XRD patterns of $SrAl_2O_4$ (a), $SrAl_2O_4$: Eu^{2+} (b) and $SrAl_2O_4$: Eu^{2+}, $Dy3^{+}$ (c). The $SrAl_2O_4$ JCPDS pattern is shown on the bottom for comparison purposes.

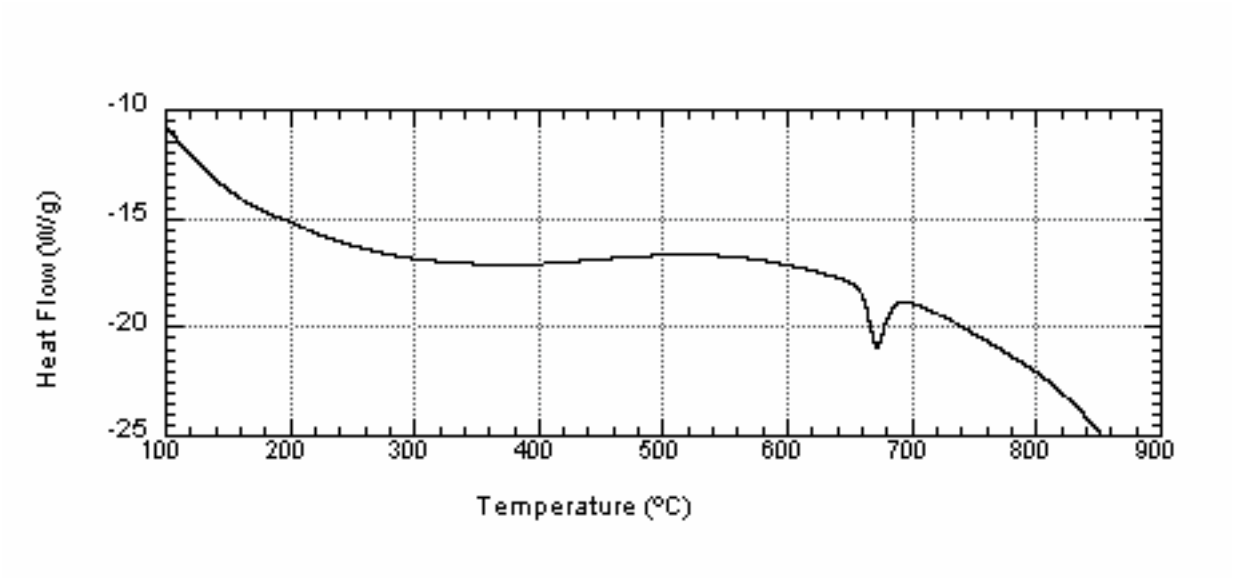

Fig. 4. DSC plot obtained for a $SrAl_2O_4$: Eu^{2+}, Dy^{3+} phosphor prepared by laser melting. The peak observed near 660 ºC is assigned to the monoclinic to hexagonal phase transition reported in the literature for this system.[21]

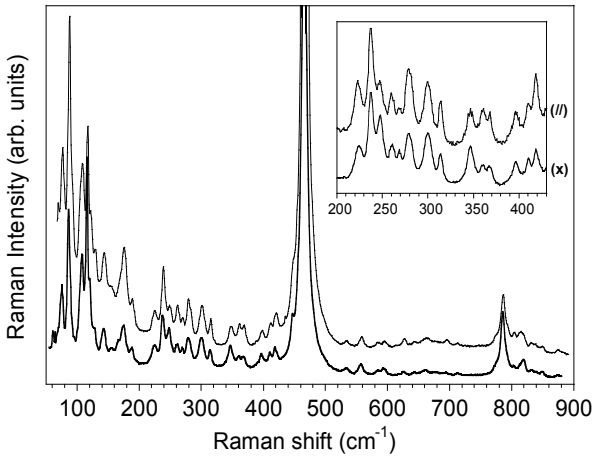

Fig. 5. Raman spectrum of laser synthesized $SrAl_2O_4$ (lower graph), compared to that of reference monoclinic $SrAl_2O_4$ produced by solid state reaction (upper graph). The inset shows the spectrum of $SrAl_2O_4$ in two different polarization configurations (see text).

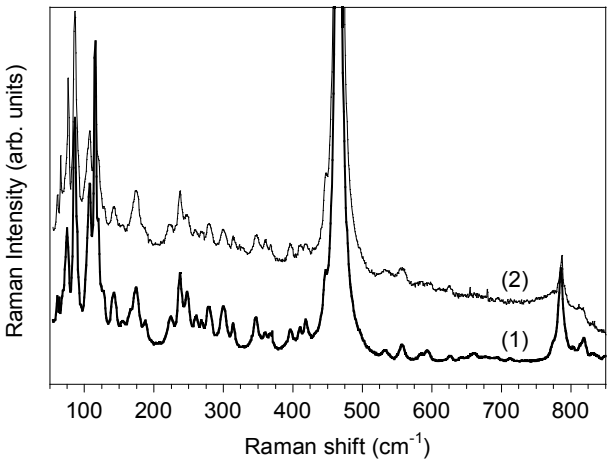

Fig. 6. Raman spectra of pure (1) and Eu, Dy doped (2) $SrAl_2O_4$ single crystals.

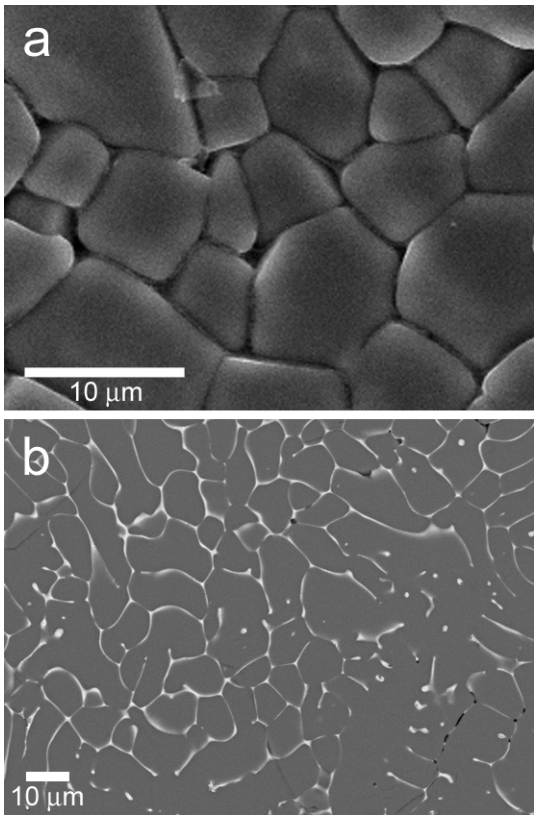

Fig. 7. SEM micrographs, secondary-electron image (a) and backscattered-electron image (b), showing the microstructure of $SrAl_2O_4$: Eu^{2+}, Dy^{3+} phosphor obtained by laser melting. Accumulation of heavier (white contrast in backscattered mode) rare earth elements at the grain boundaries is clearly distinguished in (b).

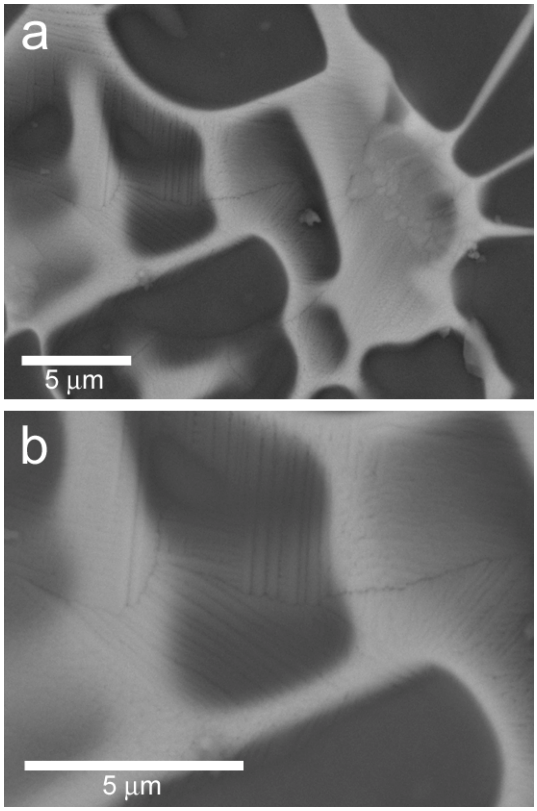

Fig. 8. SEM micrograph of unpolished $SrAl_2O_4:Eu^{2+}$, Dy^{3+} phosphor obtained by the laser melting method, showing the lamellar microstructure of the eutectic phase at different magnifications.

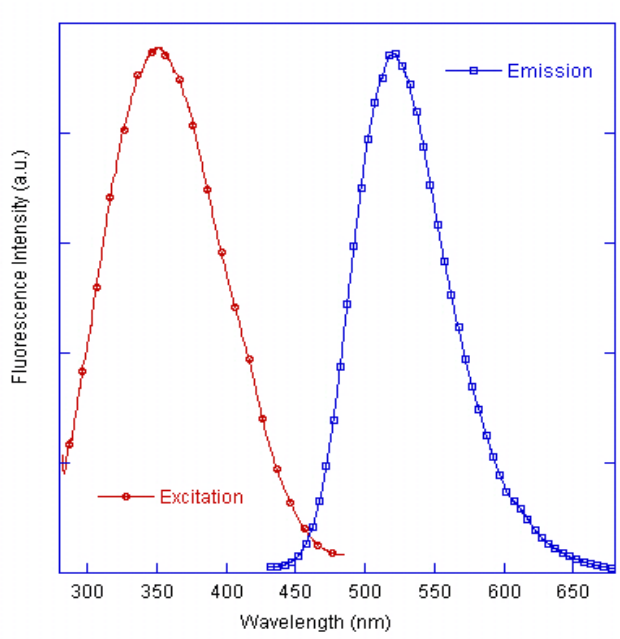

Fig. 9. Emission and excitation spectra of the $SrAl_2O_4$: Eu^{2+} phosphor.

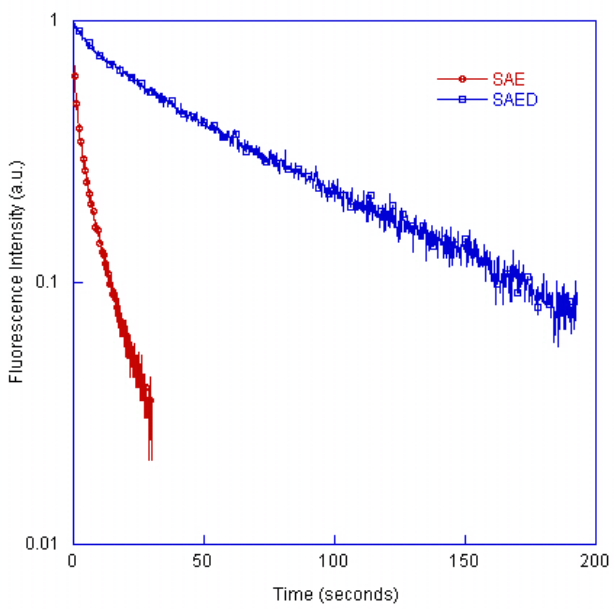

Fig. 10. Decay curves of luminescence of $SrAl_2O_4$: Eu^{2+} (SAE) and $SrAl_2O_4$: Eu^{2+}, Dy^{3+} (SAED) phosphors.